Complex balancing motions of an inverted pendulum subject to delayed feedback control

J. Sieber and B. Krauskopf

Bristol Centre for Applied Nonlinear Mathematics, Department of Engineering Mathematics, Queen's Building, University of Bristol, BS8 1TR, U.K.

Abstract

We show that an inverted pendulum that is balanced on a cart by state-dependent delayed control may exhibit small chaotic motion about the upside-down position while the velocity of the cart performs a random walk. In periodic windows associated with this chaotic regime we find periodic orbits of arbitrarily high period that correspond to complex balancing motion of the pendulum with bounded velocity of the cart. This result is obtained by studying homoclinic bifurcations of a reduced three-dimensional vector field near a triple-zero eigenvalue singularity.

Key words: inverted pendulum, balancing motion, feedback control, delay differential equation, triple-zero singularity, homoclinic tangency
PACS: 05.45, 02.30.Ks

1 Introduction

Balancing a long stick is easier than balancing a short stick. This well-known fact is due to the human reaction time which introduces the effect of a time delay into this control problem. This reaction time is about 100 ms for eye-hand coordination [1], and the effective delay time is longer the shorter the stick. In fact, any stabilization scheme using state-dependent feedback control will be adversely affected by control loop latency, that is, a non-zero reaction time between the measurement of the state of the system and the control action. Delay-induced instabilities have been studied extensively in other systems with delay, for example, in coupled neurons [2,3], lasers subject to optical feedback due to external reflections [4], and in milling processes [5].

We consider here the idealized model of balancing control, namely an inverted planar pendulum on a moving cart that is stabilized by a state-dependent control force D; see Fig. 1 and Sec. 2 for the mathematical details. Due to

the latency of the control loop, the control force takes effect only after some fixed delay τ. This leads to a mathematical description by a delay differential equation (DDE) with an infinite-dimensional phase space; see [6,7] as general references to the theory of DDEs. The DDE is symmetric with respect to reflection at the origin, the upside-down position of the pendulum, due to the reflection symmetry of the pendulum. Perfect control is achieved when the upside-down position is stable, while the cart moves with constant velocity. (This velocity at the stable limit can be brought to zero by choosing a suitable initial condition or by introducing a small amount of damping.)

Linear stability analysis shows that there is a region in the parameter space of the controller where perfect control can be achieved, provided the delay τ is not too large [8]. Furthermore, stability is generally lost in a Hopf bifurcation. It is possible to compute the criticality of this Hopf bifurcation, which gives a first idea of how the system behaves beyond the stability boundary [8–10]. If the Hopf bifurcation is supercritial then the pendulum performs (initially) small oscillations about the upside-down position but with finite velocity of the cart. Such small oscillations have been observed in experiments [10]. They are an example of a relaxed form of stabilization that we call *balancing motion* (much like what actually happens when you balance a stick). Such a balancing motion is stable and bounded around the upside-down position while the velocity of the cart is also bounded. The question arises whether there are more complex balancing motions apart from perfect stabilization and simple oscillations after the first Hopf bifurcation. Mathematically, such balancing motion corresponds to a symmetric attractor of the system with bounded velocity of the cart.

Computer-based balancing experiments have shown chaotic balancing motions with small amplitudes, referred to as micro chaos [11]. However, this dynamics is due to discontinuities associated with digital sampling in time and space. Consequently, the results in Ref. [11] left the question still open whether complex balancing motions are possible entirely within the scope of the standard (smooth) model for a controlled inverted pendulum.

Bifurcation analysis shows that any such solution, if it exists, cannot be found by simply following the bifurcations of the initial symmetric periodic orbits [12]. In particular, the simple oscillations disappear in a symmetry breaking bifurcation (pitchfork bifurcation of periodic orbits), which results in a complete loss of control [8,12]. There are now two (symmetrically related) periodic orbits. Each of these nonsymmetric periodic orbits corresponds to the pendulum wanting to fall to one side, which the controller will attempt to compensate for by increasing the velocity of the cart. Hence, the parameter region where nonsymmetric regimes are prevalent is typically not regarded as physically relevant.

In this paper we show that complex balancing motions of the inverted pen-

dulum exist inside this parameter region associated with pairs of nonsymmetric attractors. We find bounded symmetric chaotic motion of the pendulum around its upside-down position. This motion consists of long stretches where the pendulum is about to fall over to one side and the cart speeds up to compensate, following by another stretch where the pendulum is about to fall over to the other side and the cart reverses direction. The velocity of the cart performs a random walk in this case, hence it will eventually leave any bounded region. In other words, this chaotic motion is not balancing according to our definition requiring bounded velocity of the cart. However, we find stable symmetric periodic orbits of arbitrarily large period (but with bounded velocity of the cart) corresponding to complex balancing motion. The parameter islands where these balancing motions occur, so-called periodic windows in the parameter space, are not connected to the primary family of symmetric periodic orbits that emerged from the Hopf bifurcation.

We obtain these results by considering a three-dimensional vector field, derived and studied in Ref. [12], decribing the dyamics on the center manifold reduction of the system near a codimension-three triple-zero eigenvalue bifurcation. Starting from the basic bifurcation diagram presented in Ref. [12] we consider the parameter region where the primary symmetric periodic orbit is of saddle type. After the reduction to a (symmetric) local Poincaré map, this symmetric periodic orbit corresponds to a symmetric saddle fixed point with one-dimensional stable and unstable manifolds. Well established numerical algorithms [13] allow us to locate a first quadratic tangency of these manifolds. Then, the existence of infinitely many stable symmetric periodic orbits of arbitrarily large period follows from general statements on homoclinic tangencies [14] in two-dimensional maps. Furthermore, the pair of nonsymmetric attractors merges and forms a single symmetric chaotic attractor in a crisis bifurcation [15]. That these theoretical results are indeed of relevance for the original control system is demonstrated by showing examples of merging chaotic attractors and symmetric periodic orbits of long period in the full DDE.

The mechanism we describe in this paper is not specific to our particular model system, but is directly associated with the symmetric triple-zero singularity. One must expect crisis bifurcations and complicated symmetric attractors in any system that features this singularity. Interestingly, the triple-zero singularity appears to be prevalent when a control loop controlling a saddle equlibrium is subject to delay. For example, Ref. [16] investigated the inverted pendulum subject to a PMD (proportinal minus delay) controller and found the same singularity when increasing the control loop latency.

The paper is organised as follows. We first introduce the details of the mathematical model in Sec. 2 and then briefly recall in Sec. 3 the bifurcation diagram of the reduced three-dimensional vector field model near the triple-zero eigen-

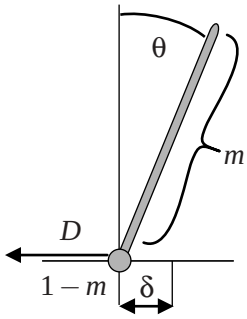

Fig. 1. Sketch of the inverted pendulum on a cart.

value bifurcation from Ref. [12]. In Sec. 4 we show that there are complex symmetric dynamics in the reduced model, and in Sec. 5 we give examples of complex balancing motion in the full control system. Finally, we conclude and point to some open problems.

2 Model equations

The dynamics of the setup in Fig. 1 are governed by the second-order differential equation for the angular displacement θ of the tip of the pendulum, which can be written in dimensionless form as

$$\left(1 - \frac{3m}{4}\cos^2\theta\right)\ddot{\theta} + \frac{3m}{8}\dot{\theta}^2\sin(2\theta) - (\sin\theta + D\cos\theta) = 0. \tag{1}$$

Here m is the mass of the uniform pendulum, $1-m$ is the mass of the cart, and D is the horizontal rescaled driving force. Due to the recscaling, time is measured in units of $\sqrt{2L/(3g)}$, where L is the length of the pendulum and g is the gravity. Because friction is not taken into account, the equation of motion for the displacement δ of the cart is decoupled from (1):

$$\ddot{\delta}(t) = L\frac{\frac{m}{2}\sin\theta\dot{\theta}^2 + \frac{2}{3}D - \frac{m}{4}\sin(2\theta)}{1 - \frac{3m}{4}\cos^2\theta}. \tag{2}$$

The force D is applied as a feedback control depending on the state of the system with the goal of stabilizing the pendulum at its upright position, which is $\theta = 0$. The feedback control force D is a function of the state of the system at some fixed time τ ago, where τ is the latency of the overall system. We study the case of a linear PD (proportional plus derivative) control force

$$D(t) = -a\theta(t-\tau) - b\dot{\theta}(t-\tau) \tag{3}$$

which is given by the control gains a and b, and features the single fixed delay time $\tau > 0$ in the controller.

By rescaling time and angular velocity the delay can be scaled to 1, and equation (1) can be written as the DDE

$$\dot{x}(t) = f(x(t), x(t-1), \lambda) \tag{4}$$

where the right-hand-side $f : \mathbb{R}^2 \times \mathbb{R}^2 \times \mathbb{R}^3 \to \mathbb{R}^2$ has the form

$$\begin{aligned} f_1(x, y, \lambda) &= x_2 \\ f_2(x, y, \lambda) &= \frac{-\frac{3}{8}m \sin(2x_1)x_2^2 + \tau^2 \sin x_1 - \cos x_1(\tau^2 a y_1 + \tau b y_2)}{1 - \frac{3}{4}m \cos^2 x_1}. \end{aligned} \tag{5}$$

Because f is odd, that is,

$$f(-x, -y, \lambda) = -f(x, y, \lambda) \tag{6}$$

the system has the symmetry of reflection in the origin. Consequently, the origin 0 is always an equilibrium, and any solution of (4)–(5) is either symmetric under this symmetry or it is nonsymmetric and its image under reflection in the origin is also a solution.

3 Center manifold reduction

In this section we summarize the results of the bifurcation analysis of a three-dimensional vector field reduction of (4)–(5) on the center manifold of a triple-zero singularity. Further details can be found in Ref. [12].

The linear stability analysis of the origin 0 depending on the parameters a, b, and τ has been performed already in Ref. [8]. There is a bounded region of stability of 0 in the (a, b)-plane if $\tau \in (0, \tau_*)$ where

$$\tau_* = \frac{1}{2}\sqrt{8 - 6m}$$

is the maximal permissible delay for stability. For $\tau \to \tau_*$ the region of linear stability shrinks to the point $a = 1$, $b = \tau_*$ and the origin 0 has a triple-zero eigenvalue singularity. At this point $\lambda_* = (1, \tau_*, \tau_*)$ the linearization of the origin has an eigenvalue 0 with algebraic multiplicity three and geometric multiplicity one.

In Ref. [12] we proved that the flow of system (4)–(5) on the local center manifold close to this singularity is governed by the three-dimensional vector

field

$$\begin{pmatrix} \dot{u}_1 \\ \dot{u}_2 \\ \dot{u}_3 \end{pmatrix} = \begin{pmatrix} 0 & 1 & 0 \\ 0 & 0 & 1 \\ -\alpha & \gamma & \beta \end{pmatrix} \begin{pmatrix} u_1 \\ u_2 \\ u_3 \end{pmatrix} + \begin{pmatrix} 0 \\ 0 \\ u_1^3 \end{pmatrix} + r^2 R(u, \mu, r) \tag{7}$$

where the $u = (u_1, u_2, u_3) \in \mathbb{R}^3$ is a new 'magnified' variable on the center subspace, R is a smooth function of its arguments and r is a small scaling parameter. Further, $\mu = (\alpha, \beta, \gamma) \in \mathbb{R}^3$ is an unfolding parameter of the singularity, defined by

$$a = 1 + \alpha \frac{1}{3} r^6, \qquad b = \tau_* + \beta \frac{\tau_*}{3} r^2, \qquad \tau = b + \gamma \frac{\tau_*}{3} r^4, \tag{8}$$

and time has been rescaled by setting $t_{\text{old}} = r^2 t_{\text{new}}$.

We now consider the truncated system, equation (7) with $r = 0$. Any hyperbolic equilibrium, periodic orbit, or normally hyperbolic invariant manifold in the truncated system persists under the small perturbation of $r^2 R$, and, hence, exists in the full DDE (4)–(5) for sufficiently small r and for the parameters obtained by (8).

Figure 2 shows a summary of the results of the bifurcation analysis of the reduced system (7) obtained by linear stability analysis in combination with numerical continuation of periodic orbits using AUTO [17]. As the truncated system (7) has cone structure one can restrict the continuation to the parameter sphere $\alpha^2 + \beta^2 + \gamma^2 = 1$, which we parametrize by φ and ψ given by

$$\alpha = \sin \frac{\pi}{2}\varphi, \qquad \beta = \cos \frac{\pi}{2}\varphi \ \cos 2\pi\psi, \qquad \gamma = \cos \frac{\pi}{2}\varphi \ \sin 2\pi\psi. \tag{9}$$

The region marked by I in Fig. 2 is the region of linear stability of 0. In the region marked by II there is a family of stable symmetric periodic orbits bifurcating from the Hopf bifurcation at 0. These periodic oscillations around the upside-down position were found in experiments in Ref. [10]. Indeed, there is only one two-parameter family of symmetric periodic orbits that is connected to the origin. It exists in a bounded region of the (φ, ψ)-plane. Its left boundary is the symmetric Hopf bifurcation of 0, the S-shaped solid curve connecting the points DZ_-, PH and DZ_+ in Fig. 2. (Note that there is also a Hopf curve of the nonsymmetric saddles between PH and DZ_+.) The right boundary is formed by global bifurcations in which the symmetric periodic orbit disappears, namely the dashed curves in Fig. 2. Along the dashed curve between DZ_- and HC there is a heteroclinic connection between the pair of nonsymmetric saddles. Along the dashed curve connecting DZ_+ and HC a homoclinic figure-eight shaped connection to 0 exists. Throughout the entire region of their existence, the symmetric periodic orbits undergo only saddle-node bifurcations and pitchfork bifurcations, where they lose their stability

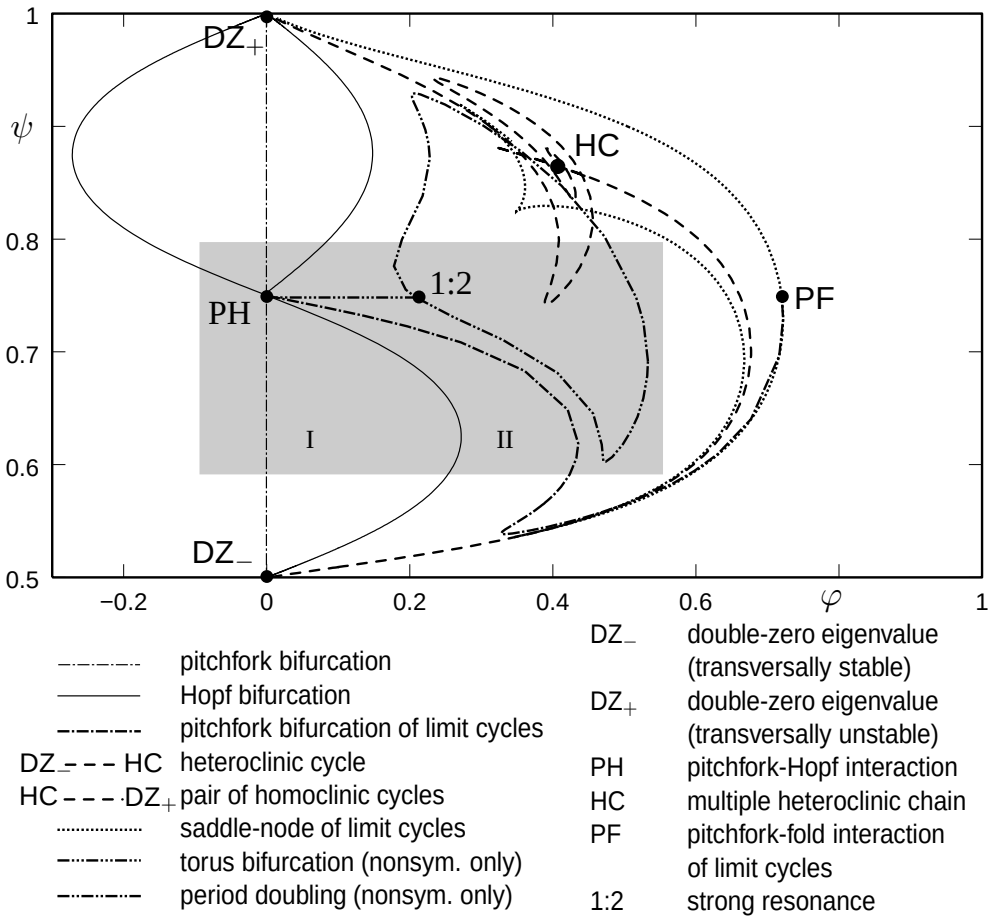

Fig. 2. Bifurcation diagram of the truncated system, system (7) for $r = 0$. The shaded area of the diagram is shown in more detail in Fig. 5.

to a branch of nonsymmetric periodic orbits. Consequently, this primary family of symmetric periodic orbits is the only non-trivial symmetric balancing regime that is 'connected' to the origin in the parameter plane, meaning that it can be found by continuation from 0.

4 Complex symmetric motion in the reduced system

The question whether there are other stable symmetric regimes, periodic or otherwise, of the truncated system (7) was already posed in Ref. [12]. As we show now, such symmetric attractors indeed exist.

The coexisting stable pair of nonsymmetric periodic orbits that branches from the primary symmetric periodic orbit at the pitchfork bifurcation (the dot-dashed boundary of region II in Figure 2) undergoes a period doubling bifurcation along the dot-dot-dashed closed curve. This is the first in an infinite

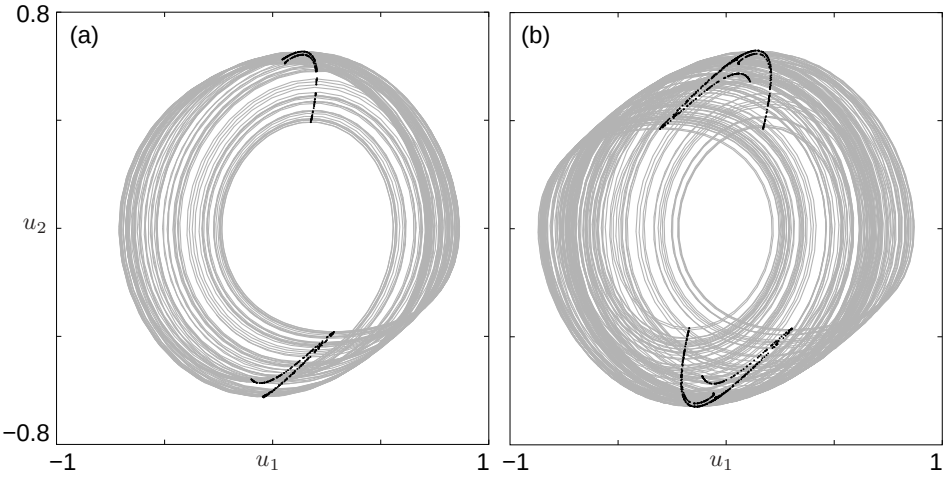

Fig. 3. One of the two coexisting nonsymmetric attractors for $(\varphi, \psi) = (0.4, 0.6958)$ (a) and the symmetric attractor for $(\varphi, \psi) = (0.4, 0.6966)$ (b) as observed in a simulation of the truncated system, (7) with $r = 0$. The intersections of the grey trajectories with the plane $\{u_3 = 0\}$ are shown as black dots.

sequence of period doubings leading to a pair of nonsymmetric chaotic attractors. Figure 3 shows two attractors in projection onto the (u_1, u_2)-plane for nearby parameter values inside the period doubling island, obtained by simulations of the truncated system, (7) for $r = 0$. While Fig. 3 (a) shows one of the two nonsymmetric chaotic attractors, Fig. 3 (b) shows a bigger symmetric chaotic attractor. It is created in a crisis bifurcation [18] that 'merges' the two nonsymmetric attractors. Roughly speaking, the attractor in panel (b) can be obtained by overlaying that in panel (a) with its symmetric counterpart, obtained by rotating panel (a) by π. Also shown in Fig. 3 are the intersection points (in black) of the attractors with the plane $\{u_3 = 0\}$. Each attractor intersects this plane in two locations, one for positive and one for negative u_2. The symmetric attractor in this section in Fig. 3 (b) consists of the two nonsymmetric pieces of the nonsymmetric attractor in Fig. 3 (a).

We will now give a more precise statement about this mechanism in terms of a homoclinic bifurcation of the Poincaré map to a section, which we choose to be $\{u_3 = 0\}$. This will also allow us to show that stable symmetric periodic orbits exist near symmetric chaotic attractors in so-called periodic windows. These symmetric periodic orbits correspond to complex balancing motion of the pendulum.

As was shown in Fig. 3 the attractors intersect the section $\{u_3 = 0\}$ transversally and in two distinct regions. We define by Π the return map of the flow of the truncated system (7) from each of these regions back to the same region. In other words, the map Π is defined as the second return to the section. The primary symmetric periodic orbit intersects the section in two points transversally along the curve of pitchfork bifurcations; see Fig. 2. Hence, the Poincaré

map Π is a well defined two-dimensional diffeomorphism in its domain of definition, the two regions as defined above. (Note that Π cannot be extended to a global Poincaré map on the entire plane $\{u_3 = 0\}$.) Because the section $\{u_3 = 0\}$ was chosen to contain the origin, the map Π inherits the odd symmetry (6) from the flow. Consequently, we can concentrate on Π in one of the two regions, say, on that for negative u_2. In this region there is a unique fixed point S corresponding to the primary symmetric periodic orbit. After the pitchfork bifurcation (to the right of the dot-dashed curve in Fig. 2) S is a saddle with eigenvalues Λ_1 and Λ_2 satisfying $0 < \Lambda_2 < \Lambda_1\Lambda_2 < 1 < \Lambda_1$. Hence, it has one-dimensional stable and unstable invariant manifolds, $W^s(S)$ and $W^u(S)$, respectively.

To show that these manifolds undergo a first quadratic homoclinic tangency we compute appropriate finite parts of these manifolds up to a prescribed accuracy. We use the algorithm from Refs. [13,19] in the form of an extension module [20] that works as part of the Tcl/TK version of the package DsTool [21]. The return map Π is computed by integration of the vector field with a Runge-Kutta fourth order discretization.

Figure 4 shows conclusive evidence that there is indeed a first quadratic tangency, which is crossed with positive velocity under variation of the parameter ψ. Panels (a) to (c) show the fixed point S, one side of its stable manifold $W^s(S)$ and both sides of its unstable manifold $W^u(S)$ for fixed $\varphi = 0.4$ and three different, but close values of ψ. Clearly, $W^s(S)$ and $W^u(S)$ do not intersect in panel (a), but do intersect in panel (c). Because finite initial pieces of these manifolds depend smoothly on parameters, these numerical results provide accurate evidence that a first tangency exists and where it is located. Panel (b) shows the approximate moment of tangency. Figure 4 (d) is the result of a long-time simulation of Π (after discarding transients) showing an attractor resembling the closure of both parts of $W^u(S)$ for the same parameter values as Fig. 4 (c).

The importance of the first tangency is that it corresponds to an attractor crisis that creates a single symmetric chaotic attractor of Π by merging two smaller nonsymmetric chaotic attractors. Before the tangency there are two distinct chaotic attractors of Π, one on each side of the shown branch of $W^s(S)$, consisting of the closure of the respective branch of $W^u(S)$. However, after the tangency it is possible to pass from one side of $W^s(S)$ to the other. This mechanism creates a single attractor and is often referred to as a crisis bifurcation [18]. More specifically, this is a symmetry-restoring (interior) crisis in which two symmetrically related attractors hit the boundary of their basin of attraction simultaneously and merge. It occurs if $W^u(S)$ and $W^s(S)$ have a homoclinic tangency and the union of the nonsymmetric attractors are equal to the closure of the whole unstable manifold $W^u(S)$ at the moment of tangency. This phenomenon was classified as intermittent switching in Ref. [15]. It was

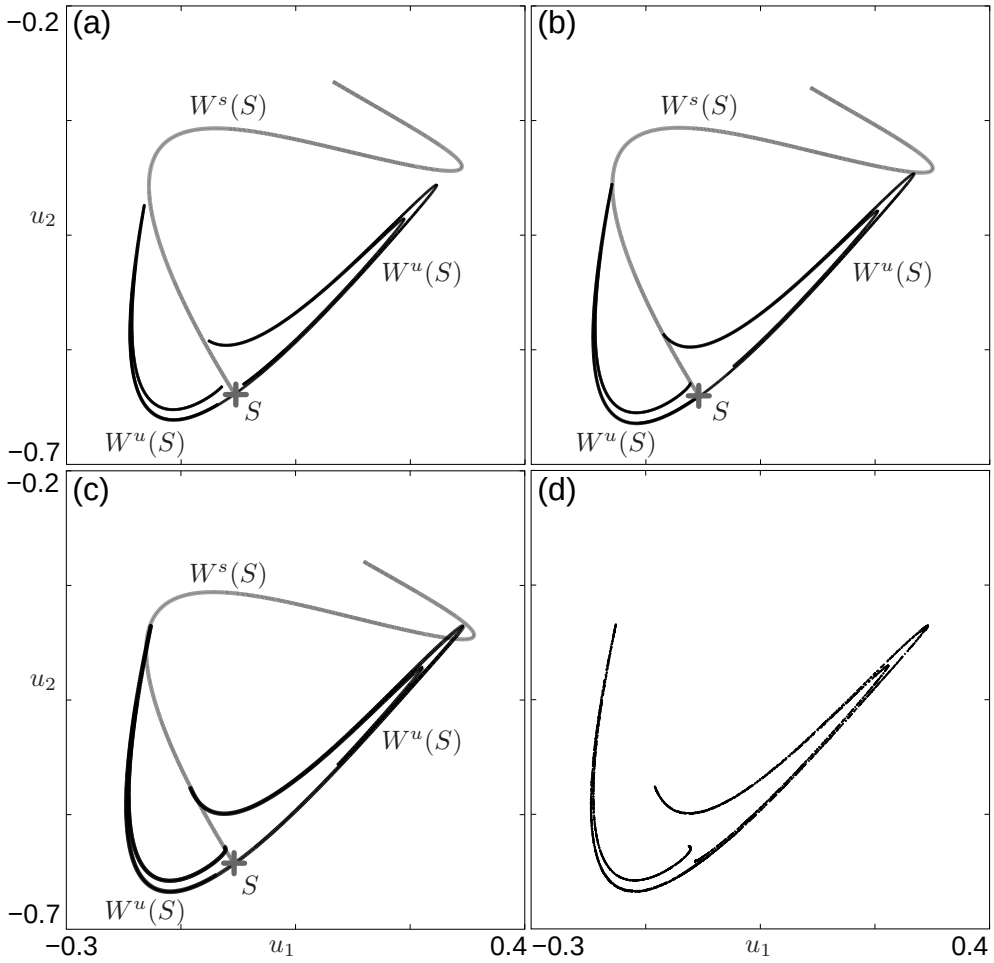

Fig. 4. Unstable and stable manifolds of S for the map Π at the parameter values $\varphi = 0.4$, (a) $\psi = 0.6950$, (b) $\psi = 0.6958$, and (c) $\psi = 0.6966$. Panel (d) shows the result of a long term simulation of Π for $\psi = 0.6966$, corresponding to the arrangement of the invariant manifolds in panel (c).

observed for expample in Ref. [22] in a DDE model (also with $\mathbb{Z}_2$-symmetry) of a laser with phase-conjugate feedback.

The dynamics on the symmetric chaotic attractor follow one of the two subparts for a long time before crossing $W^u(S)$ to then follow the other part, before switching back, and so on. This corresponds to the inverted pendulum making small chaotic oscillations while leaning to one side at a time. The pendulum does not fall over because the controller compensates by increasing the velocity of the cart, then changing direction and so on. In other words, the velocity of the cart performs a random walk.

To make rigorous statements about the existence of complicated symmetric periodic orbits of Π in the vicinity of the homoclinic tangency we perform a symmetry reduction for Π as follows. Let us denote by $\widehat{\Pi}$ the first first-return to the section composed with the symmetry operation of rotation by π. Then

$\widehat{\Pi}$ is a diffeomorphism in the same domain of definition as Π, but it does not have reflectional symmetry in the origin. In particular, the map $\widehat{\Pi}$ satisfies

$$\left(\widehat{\Pi}\right)^2 = \widehat{\Pi} \circ \widehat{\Pi} = \Pi.$$

This means that symmetric periodic orbits of Π correpond to periodic orbits of $\widehat{\Pi}$ with odd period. Similarly, nonsymmetric periodic orbits of Π are periodic orbits of even period of $\widehat{\Pi}$.

In particular, S is a fixed point, that is, a point of odd period of $\widehat{\Pi}$. The pitchfork bifurcation of S for Π corresponds to a period doubling bifurcation of S for $\widehat{\Pi}$. After this period doubling, S is a saddle fixed point of $\widehat{\Pi}$. The one-dimensional stable and unstable invariant manifolds of S with respect to $\widehat{\Pi}$ and Π are identical. Thus, we denote them by $W^u(S)$ and $W^s(S)$ for $\widehat{\Pi}$ as well.

The existence of the quadratic tangency of $W^u(S)$ and $W^s(S)$ allows us to apply the well-established theory of homoclinic tangencies in two-dimensional diffeomorphisms; see, for example, Ref. [14]. The saddle value of S in for the parameter values of Fig. 4(c) is less than 1, that is, the eigenvalues Λ_j $(j = 1, 2)$ of $\widehat{\pi}$ at S satisfy the relation

$$\Lambda_1 < -1 < \Lambda_1\Lambda_2 < 0 < \Lambda_2 < 1. \tag{10}$$

The following lemma is an immediate consequence of the general theoretical results [14] for two-dimensional diffeomorphisms close to homoclinic tangencies for saddle fixed points satisfying relation (10).

Lemma 1 *Close to the homoclinic tangency there exist infinitely many open sets of parameters ψ where the map $\widehat{\Pi}$ has stable periodic orbits with odd period.*

Indeed, the general results are much deeper stating that there exist infinitely many stable periodic orbits simultaneously for residual sets in the so called Newhouse regions of the parameter space. We remark that [14] assumes that the map is orientation preserving, which $\widehat{\Pi}$ is not. However, this assumption is not actually necessary for the construction of the stable periodic orbits.

Although these periodic orbits typically have a large period and a small basin of attraction, they are robust with respect to small perturbations of the map. Hence, they exist as symmetric periodic orbits in the non-truncated system (7) and in the full DDE system (4)–(5) as well. Any of these periodic orbits corresponds to a symmetric small-amplitude regime in (4)–(5) with a periodic and, hence, bounded velocity of the cart. In other words, we have found many balancing motions of the inverted pendulum that are given by these more complex symmetric periodic orbits.

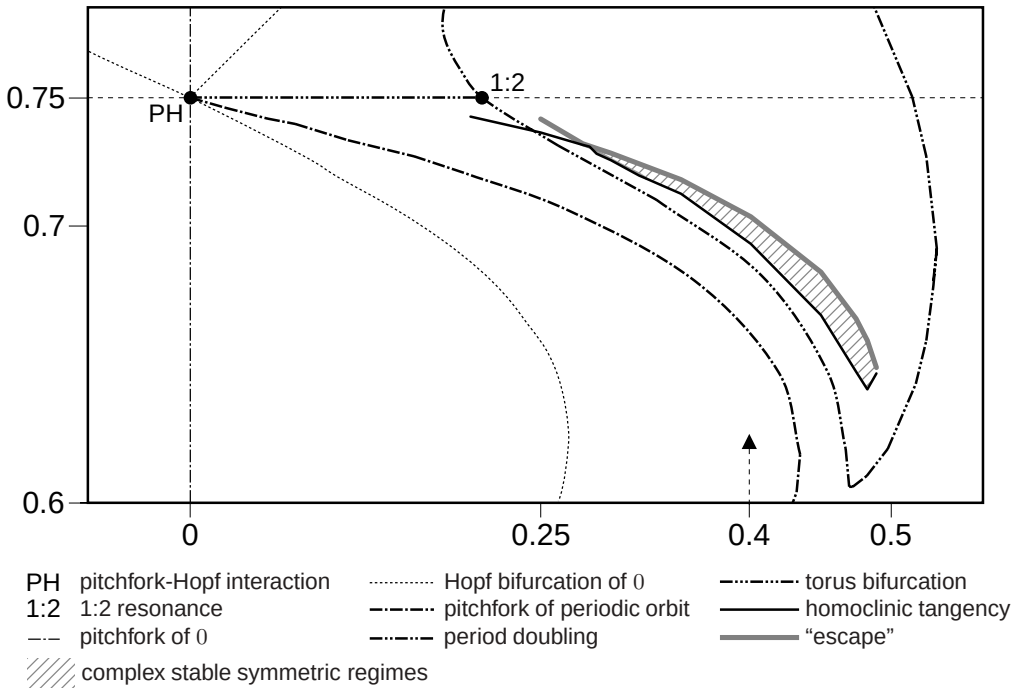

Fig. 5. Curve of homoclinic tangency and the region of stable symmetric attractors in the bifurcation diagram. The arrow shows the line along which we chose the parameter values for Figs. 3, 4 and 6.

The homoclinic tangency of Π (and $\widehat{\Pi}$) to S forms a smooth curve in the (φ, ψ)-plane that is robust with respect to small perturbations, for example, small nonzero r in (7) or numerical errors. In Figure 5 we have added as a solid black polyon an approximation of the curve of homoclinic tangency to S to the bifurcation diagram. The corners of this polygon have been found by identifying the first homoclinic tangency up to 4 digits in φ and ψ. Since the saddle value of S is negative along the whole curve, Lemma 1 implies that there exist many regions near the curve of homoclinic tangency where symmetric stable periodic orbits exist.

If the nonsymmetric attractors of Π are equal to the closure of the whole unstable manifold $W^u(S)$ at the curve of homoclinic tangency, one observes an attractor crisis [18] as depicted in Fig. 3 and Fig. 4(d). This defines one boundary of the region in the (φ, ψ)-plane where chaotic symmetric attractors may occur. A numerical approximation of this region is hatched in Fig. 5. Its other boundary is defined by the occurence of a pair of (symmetrically related) heteroclinic tangencies between S and the pair of nonsymmetric saddle equilibria $E_\pm = (\pm\sqrt{\sin(\pi\varphi/2)}, 0, 0)$ of the truncated system (7). The saddles $E_\pm$ both have a two-dimensional stable manifold $W^s(E_\pm)$. The intersections of these stable manifolds with the plane $\{u_3 = 0\}$ generically are curves that establish the boundary between bounded dynamics of Π and escape to infinity. Consequently, a tangency between $W^u(S)$ and $W^s(E_+)$ (and simultaneously

between $W^u(S)$ and $W^s(E_-)$) is a codimension-one bifurcation that defines the boundary of the parameter region where Π can have stable bounded regimes. The heteroclinic tangency forms a smooth curve in the (φ, ψ)-plane, which we approximated by the thick gray polygon in Figure 5. The corners were found by checking the boundedness of a numerical trajectory over large integration times. We started simulations in the vicinity of the nonsymmetric fixed points of Π and checked whether the orbit escapes to infinity within 15000 iterates of Π. (Note that the return map Π is not well defined near the saddles $E_\pm$, so that algorithms for computing one-dimensional manifolds cannot be readily applied.)

We remark that, at the moment of the homoclinic tangency, the (chaotic) nonsymmetric attractors may be substantially smaller than the closure of the unstable manifold $W^u(S)$. In this case, there is no attractor crisis at the tangency, but a change in the basin of attraction of the nonsymmetric attractor (also referred to as a basin boundary metamorphosis [18]). This happens along the part of the black solid tangency curve in Fig. 5 that does not bound the shaded region, to the left of the codimension-two point where the black and grey curves meet. (This point appears to be what is known as a double crisis vertex [23] in systems without symmetry.) In fact, the tangency curve even crosses the period doubling curve (for $\varphi < 0.25$), so that the homoclinic tangency takes place when the two nonsymmetric fixed points of Π are stable.

5 Complex symmetric motion in the full DDE system

The center manifold reduction performed in Ref. [12] guarantees that all phenomena observed in the truncated system (7) that are robust with respect to small perturbations are also present in the full DDE system (4)–(5). Furthermore, in Ref. [12] we could establish a very good quantitative agreement between the bifurcation diagrams of the truncated system and that of the full DDE system even quite far away from the triple-zero singularity. On the other hand, symmetric chaotic attractors of Π are not robust in this sense, and the complex stable symmetric periodic orbits, while being robust according to Lemma 1, may have extremely small bassins of attraction and are typically difficult to find. Hence, the question arises whether we can observe the phenomena described in section 4 in the full DDE system (4)–(5) as well.

To confirm this, we set the scaling parameter to $r = 0.5$ and the mass of the pendulum to $m = 0$. (Note that m only enters in the formula for τ^*.) To convert the parameters φ and ψ back to the original parameters a, b, and τ we use the scaling (8). We simulate the full DDE system (2), (4)–(5) for x and δ using a 4th-order fixed step Adams-Bashforth method with a stepsize of 0.05.

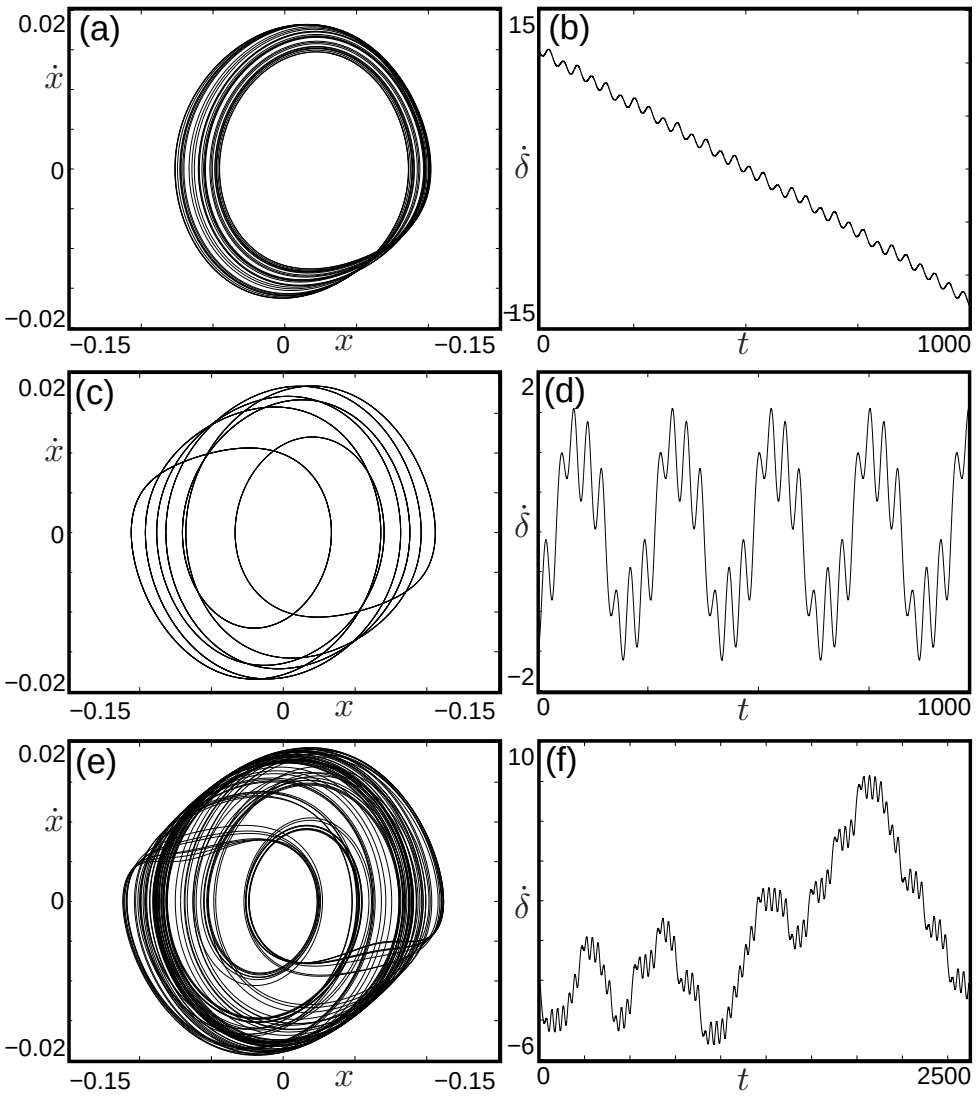

Fig. 6. Simulation results for DDE system (4)–(5) with $m = 0$ demonstrating the transition to symmetric attractors. The upper row shows the projection into the (x_1, x_2)-plane, the lower row shows the time trace of the velocity of the cart $\dot{\delta}$. Parameter values are $\varphi = 0.4$ and $\psi = 0.702$ for (a), (b), $\psi = 0.705$ for (c), (d), and $\psi = 0.71$ for (e), (f).

Figure 6 shows simulation results for three different parameter values near $(\varphi, \psi) = (0.4, 0.7)$, after discarding a transient of duration 5000. Three different regimes are shown in the $(x(t), \dot{x}(t))$-projection in the first column and as the corresponding time profile of the cart velocity $\dot{\delta}(t)$ in the second column. Panel (a) shows a nonsymmetric chaotic attractor, which does not correspond to successful balancing since $|\dot{\delta}(t)|$ increases on average according to panel (b). Panel (c) shows a complicated symmetric periodic orbit. It corresponds to successful balancing motion because $\dot{\delta}(t)$ remains bounded as can be seen from panel (d). Finally, panel (e) shows a symmetric chaotic attractor, for

which the cart velocity performs a random walk with a constant mean; see panel (f). The velocity will eventually leave any bounded region. In summary, Fig. 6 shows that the symmetric attractors that exist in the reduced system according to Lemma 1 can indeed be found in numerical simulations of the full DDE. In particular, complex balancing motion due to complicated symmetric periodic orbits exists even quite far away from the triple-zero singularity.

6 Discussion and conclusions

The controlled inverted pendulum is a model case for investigating nonlinear phenomena due to delay-induced instabilities. Previous [1,8,16] and recent [10,12] studies considered the linear stability of the origin and found a primary family of small-scale (symmetric) periodic balancing motions branching off in a Hopf bifurcation. The results presented in this paper show that more complex balancing motions are possible and supported even by the simplest possible model for pendulum motion with control. The basic mechanism for this behavior is a homoclinic tangency of the primary symmetric periodic orbit, allowing two nonsymmetric attractors to collide and form a bigger symmetric attractor. Since this mechanism was found in the truncated normal form of the symmetric triple-zero singularity it is not specific to the inverted pendulum with a delayed PD controller that we studied in this paper. Indeed we expect the emergence of complex symmetric attractors in many other systems — in particular, in other symmetric control problems with delay.

A characteristic feature of the complex balancing motions described in this paper is that they are located in islands in the parameter space that are isolated from the stability regions of the origin and the primary periodic orbits. While some of these islands may be big enough to be accessible experimentally, they will be difficult to find experimentally (it was already difficult to find them in the model) because they cannot simply be reached by following a known solution under variation of a parameter. Finding complex balancing regimes in an experiment is a challenging open problem.

A related open question is whether the more complex phenomena described in this paper and in Ref. [12] can also be found in more realistic balancing models. For example, the model compared with the experiments in Ref. [10] included viscous friction and a component of the control force D depending on the displacement δ and the velocity $\dot{\delta}$ of the cart (in order to keep δ near 0). This is an interesting and challenging question because even small friction and a weak dependence of D on δ and $\dot{\delta}$ are singular perturbations of (1)–(2).

Acknowledgments

The research of J.S. is supported by EPSRC grant GR/R72020/01 and that of B.K. by an EPSRC Advanced Research Fellowship.

References

[1] J. L. Cabrera, J. G. Milton, On-off intermittency in a human balancing task, Physical Review Letters 89 (2002) 158702.

[2] C. M. Marcus, R. M. Westervelt, Stability of analog networks with delay, Phys. Rev. A 39 (1989) 347–359.

[3] L. P. Shayer, S. A. Campbell, Stability, bifurcation, and multistability in a system of two coupled neurons with multiple time delays, SIAM J. of Appl. Math. 61 (2) (2000) 673–700.

[4] B. Krauskopf, D. Lenstra (Eds.), Fundamental Issues of Nonlinear Laser Dynamics, American Institute of Physics, 2000.

[5] F. C. Moon, Dynamics and Chaos in Manufacturing Processes, Wiley, New York, 1998.

[6] J. K. Hale, S. M. V. Lunel, Introduction to Functional Differential Equations, Vol. 99 of Applied Mathematical Sciences, Springer-Verlag, 1993.

[7] O. Diekmann, S. van Gils, S. M. V. Lunel, H.-O. Walther, Delay Equations, Vol. 110 of Applied Mathematical Sciences, Springer-Verlag, 1995.

[8] G. Stépán, Retarded Dynamical Systems: Stability and Characteristic Functions, Longman Scientific and Technical, 1989.

[9] S. A. Campbell, J. Bélair, Analytical and symbolically-assisted investigation of Hopf bifurcation in delay-differential equations, Canadian Applied Mathematics Quarterly 3 (2) (1995) 137–154.

[10] M. Landry, S. A. Campbell, K. Morris, C. Aguilar, Dynamics of an inverted pendulum with delayed feedback control, Preprint, University of Waterloo, submitted (2003).

[11] G. Haller, G. Stépán, Micro-chaos in digital control, J. Nonlinear Sci. 6 (1996) 415–448.

[12] J. Sieber, B. Krauskopf, Bifurcation analysis of an inverted pendulum with delayed feedback control near a triple-zero eigenvalue, Nonlinearity 17 (1) (2004) 85–104.

[13] B. Krauskopf, H. M. Osinga, Growing 1D and quasi 2D unstable manifolds of maps, J. Comp. Phys. (146) (1998) 404–419.

[14] J. Palis, F. Takens, Hyperbolicity and sensitive chaotic dynamics at homoclinic bifurcations, Cambridge studies in advanced mathematics, Cambridge University Press, 1993.

[15] C. Grebogi, E. Ott, F. Romeiras, J. Yorke, Critical exponents for crisis-induced intermittency, Phys. Rev. A 36 (11) (1987) 5365–5380.

[16] F. M. Atay, Balancing the inverted pendulum using position feedback, Appl. Math. Letters 12 (1999) 51–56.

[17] E. J. Doedel, A. R. Champneys, T. F. Fairgrieve, Y. A. Kuznetsov, B. Sandstede, X. Wang, AUTO97, Continuation and bifurcation software for ordinary differential equations (1998).

[18] K. Alligood, T. Sauer, J.A. Yorke, Chaos: An Introduction to Dynamical Systems, Springer, New York, 1997.

[19] B. Krauskopf, H. M. Osinga, Investigating torus bifurcations in the forced Van der Pol oscillator, in: E. Doedel, L. Tuckerman (Eds.), Numerical Methods for Bifurcation Problems and Large-Scale Dynamical Systems, Vol. 119 of IMA Vol. Math. Appl., Springer-Verlag, 2000.

[20] J. England, B. Krauskopf, H. Osinga, Computing one-dimensional stable manifolds of planar maps without the inverse, Preprint 2003.02, University of Bristol, Bristol Centre for Applied Nonlinear Mathematics (2003).

[21] A. Back, J. Guckenheimer, M. Myers, F. Wicklin, P. Worfolk, DsTool: computer assisted exploration of dynamical systems, Notices Amer. Math. Soc. 39 (4) (1992) 303–309.

[22] B. Krauskopf, G.R. Gray, D. Lenstra, Semiconductor laser with phase-conjugete feedback: dynamics and bifurcations, Phys. Rev. E 58 (1998) 7190–7197.

[23] H.B. Stewart, Y. Ueda, C. Grebogi, J.A. Yorke, Double crises in two-parameter dynamical systems, Phys. Rev. Lett. 75(13) (1995) 2478–2481.